Design, synthesis, biological evaluation and molecular docking studies of phenylpropanoid derivatives as potent anti-hepatitis B virus agents

ARTICLE *in* EUROPEAN JOURNAL OF MEDICINAL CHEMISTRY · MAY 2015

Impact Factor: 3.45 · DOI: 10.1016/j.ejmech.2015.03.056

7 AUTHORS, INCLUDING:

Wanxing Wei
Guangxi University
19 PUBLICATIONS **64** CITATIONS

SEE PROFILE

European Journal of Medicinal Chemistry 95 (2015) 473–482

Contents lists available at ScienceDirect

European Journal of Medicinal Chemistry

journal homepage: http://www.elsevier.com/locate/ejmech

Original article

Design, synthesis, biological evaluation and molecular docking studies of phenylpropanoid derivatives as potent anti-hepatitis B virus agents

Sheng Liu [a], Wanxing Wei [a, *], Yubin Li [b], Xu Liu [a], Xiaoji Cao [c], Kechan Lei [a], Min Zhou [a]

[a] Department of Chemistry, Guangxi University, Nanning 530004, PR China
[b] School of Chemistry and Chemical Engineering, Sun Yat-Sen University, Guangzhou 510275, PR China
[c] Center of Analysis and Testing, Zhejiang University of Industry, Hangzhou 310014, PR China

ARTICLE INFO

Article history:
Received 5 November 2014
Received in revised form
24 March 2015
Accepted 25 March 2015
Available online 27 March 2015

Keywords:
Synthesis
Phenylpropanoid derivatives
Anti-HBV activity
Structure–activity relationships
Molecular docking

ABSTRACT

A series of phenylpropanoid derivatives were synthesized, and their anti-hepatitis B virus (HBV) activity was evaluated in HepG 2.2.15 cells. Most of the synthesized derivatives showed effective anti-HBV activity. Of these compounds, compound 4c-1 showed the most potent anti-HBV activity, demonstrating potent inhibitory effect not only on the secretion of HBsAg (IC_{50} = 14.18 μM, SI = 17.85) and HBeAg (IC_{50} = 6.20 μM, SI = 40.82) secretion but also HBV DNA replication (IC_{50} = 23.43 μM, SI = 10.80). The structure–activity relationships (SARs) of phenylpropanoid derivatives had been discussed, which were useful for phenylpropanoid derivatives to be explored and developed as novel anti-HBV agents. Moreover, the docking study of all synthesized compounds inside the HLA-A protein (PDB ID: 3OX8) active site were carried out to explore the molecular interactions and a molecular target for activity of phenylpropanoid derivatives with the protein using a moe-docking technique. This study identified a new class of potent anti-HBV agents.

1. Introduction

Hepatitis B virus (HBV) infection is a serious worldwide health problem, which can cause both acute and chronic infections of the liver and may lead to lifelong infection, cirrhosis, hepatocellular carcinoma, liver failure, or death [1,2]. There are about 350–400 million people worldwide are chronically infected with HBV with 0.5–1.2 million global deaths per year [3]. Currently, therapies including immunomodulator, interferons (interferon-alpha and pegylated interferon), and nucleoside drugs (lamivudine, adefovir dipivoxil, entecavir, telbivudine and tenofovir) for treating HBV are still unsatisfactory, due to high recurrence, drug resistance and inevitable side effects [4]. Therefore, there exists a significant unmet medical need to explore novel classes of drugs with different antiviral targets and mechanisms for anti-HBV purposes.

Natural products and their derivatives possessing various skeletons could provide a great opportunity for finding novel HBV inhibitors [5–9]. In our continuing research for *Phyllanthus niruri* L., a traditional Chinese medicinal herb used in folk medicine for liver protection and antihepatitis B, anti-HBV active constituents, such as niranthin, nirtetralin, nirtetralin A and nirtetralin B, were investigated [10–12]. In view of their novel structural template, which differs from those of all reported anti-HBV agents, we designed and synthesized a series of analogs in order to screen and determine structure–activity relationships (SARs) and develop more potent anti-HBV agents. As the facts that the anti-HBV active lignans possess the same structural fragment, 3,4-dimethoxyphenyl, 3,4,5-trimethoxyphenyl, benzo[d][1,3]dioxol-5-yl, or 4-methoxybenzo[d][1,3]dioxole-5-yl, in their molecular structures, we selected (E)-3-(3,4-dimethoxyphenyl)acrylic acid (a), (E)-3-(3,4,5-trimethoxyphenyl)acrylic acid (b), (E)-3-(benzo[d][1,3]dioxol-5-yl) acrylic acid (c) and (E)-3-(7-methoxybenzo[d][1,3]dioxol-5-yl) acrylic acid (d) as the main scaffold for the design and synthesis of novel compounds as potent anti-HBV agents. According to molecular hybridization principle, esterification of natural compounds is an effective approach for achieving promising derivatives, by which two active parts can be easily hybridized to enhance activity [13,14]. Some derivatives of the four acrylic acids were synthesized for treatment of HIV, antiproliferative activity, antioxidation and antitumor activity [15–18], and some non-nucleoside anti-HBV agents such as isoflavone analogs also have been reported [19–21], but no investigation was concerned with phenylpropanoid analogs for HBV activity. Consequently, our efforts were devoted to design,

* Corresponding author.
E-mail address: wxwei@gxu.edu.cn (W. Wei).

http://dx.doi.org/10.1016/j.ejmech.2015.03.056
0223-5234/

synthesize, pharmacological evaluation in vitro and SARs elucidation of a series of phenyl acryloyl type oxime esters based on the four acrylic acids as anti-HBV agents.

A QSAR study was carried out for all the series of molecules to help in early preclinical development and avoid costly late-stage preclinical [22,23]. In addition, attempt to elucidate the molecular interactions and a molecular target for activity was achieved by molecular docking of all synthesized compounds into the active site using molecular operating environment (MOE).

2. Results and discussion

2.1. Chemistry

General synthesis for the intermediate and target compounds is depicted in Scheme 1. Substituted benzaldehyde was reacted with hydroxylamine hydrochloride in EtOH in the presence of sodium acetate to yield oxime 1–3 in a good yield [24]. Intermediates 2a–d were prepared by Knoevenagel condensation of malonic acid and the aldehyde group of four benzaldehydes with yields of 80%–90% [25]. The final oxime ester derivatives (4a-1 ~ 4a-3), (4b-1 ~ 4b-3), (4c-1 ~ 4c-3), (4d-1 ~ 4d-3) were obtained by reaction of oxime with cinnamoyl chloride 3a–d in the presence of TEA, which was obtained by reaction of substituted phenylacrylic acid 2a-d and thionyl chloride in DCM [26].

The structures of the newly synthesized compounds (4a-1 ~ 4a-3), (4b-1 ~ 4b-3), (4c-1 ~ 4c-3), (4d-1 ~ 4d-3) were characterized by ^{1}H NMR, ^{13}C NMR and MS data and their data are presented in the experimental section. ^{1}H NMR spectra of the derivatives showed a singlet at about 8.35–8.76 ppm corresponding to N=CH proton. Two doublets at 6.37–6.74 and 7.53–7.84 ppm with J = 15.25–15.91 Hz corresponding to trans hydrogens of CH=CH respectively. The singlet at 3.89–3.96 ppm attributed to O–CH_3 protons, and at 6.00–6.04 corresponded to OCH_2O protons. The chemical shifts of aromatic hydrogens of the phenyl ring appeared as multiplets in the region δ 6.67–7.21. ^{13}C NMR chemical shifts for title compounds were observed in their expected regions. ^{13}C NMR spectrum for the derivatives showed signals at 55.26–61.00, 101.45–102.12, 155.15–160.04 and 162.31–165.92 corresponding to CH_3, CH_2, C=N and C=O, respectively.

2.2. QSAR study

The 3D structures of all the compounds were generated using the Built Optimum option of Hyperchem software (version 8.0), and subsequently energy minimized using MM + force field. Then, the structures were fully optimized. Molecular descriptors were determined by QSAR study, including logP, molar refractivity, surface area, volume, hydration energy and polarizability, and the results showing that all molecules have drug like properties (Table 1). All the compounds have the molecular weight ranging from 285 to 350 Da. The log P values of these compounds are superior to act as drug which is −2.14 to 0.80 and the molar refractivity is in the range of 80–100.

2.3. Molecular docking

Molecular docking studies of phenylpropanoid derivatives were

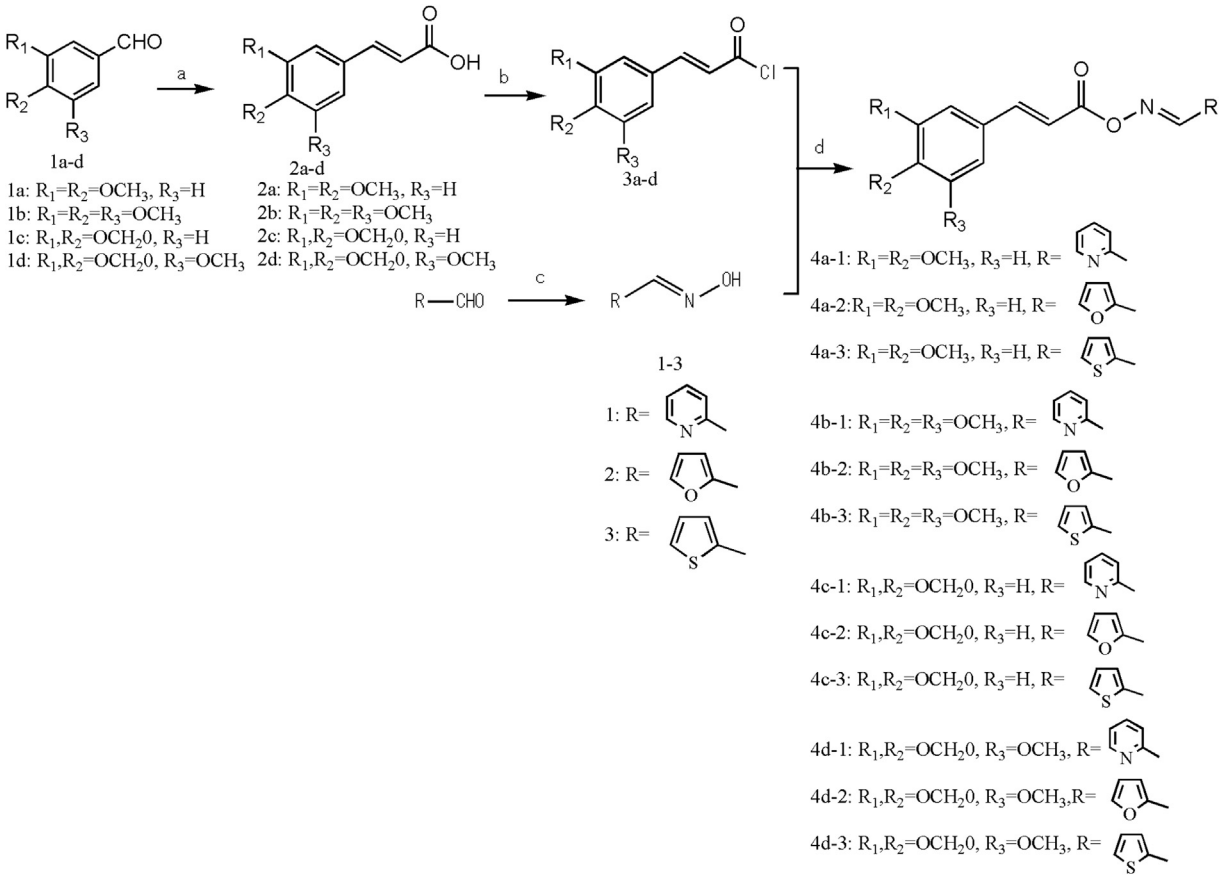

Scheme 1. Synthetic route to the series of compounds. Reagents and conditions: (a) $CH_2(COOH)_2$, piperidine, C_5H_5N, reflux, 4 h, 80–90%; (b) $SOCl_2$, CH_2Cl_2, reflux, 5 h, 95%; (c) H_2NOH–HCl, AcONa, EtOH, 60 °C, 1 h, 98%; (d) Et_3N, CH_2Cl_2, rt, 12 h, 50–70%.

Table 1
Molecular descriptors of derivatives from QSAR study.

Ligand	Molecular weight (Da)	LogP	Molar refractivity (Å^3)	Surface area (Å^2)	Volume (Å^3)	Hydration energy (kcal/mol)	Polarizability (Å^3)
3TC	229.25	−0.55	55.14	525.55	606.87	48.20	21.71
4a-1	312.32	0.61	93.01	704.41	912.63	43.90	33.13
4a-2	317.36	−1.08	90.78	729.25	898.62	47.75	32.20
4a-3	317.36	−0.81	93.60	709.11	904.30	44.77	33.36
4b-1	342.35	−0.38	99.38	757.97	974.66	43.66	35.61
4b-2	331.32	−2.14	93.53	756.01	944.36	43.13	33.47
4b-3	347.39	−1.80	99.98	762.65	966.33	44.54	35.84
4c-1	296.28	0.80	85.85	715.19	837.91	41.55	30.52
4c-2	285.25	−0.96	80.00	713.15	807.65	41.03	28.39
4c-3	301.32	−0.62	86.44	719.87	829.56	42.42	30.76
4d-1	326.3	−0.19	92.22	761.65	907.50	40.43	33.00
4d-2	315.28	−1.95	86.37	759.71	877.24	39.90	30.86
4d-3	331.34	−1.61	92.82	766.32	899.14	41.31	33.23

carried out using MOE 2008.10 as docking software in order to rationalize biological activity results and understand the various interactions between ligand and protein in the active site in detail. The crystal structure of HLA-A protein (PDB ID: 3OX8), which was associated with severe liver inflammation in Chinese patients with chronic HBV infection, was used for docking study. And the 'Site Finder' tool of the program was used to search for its active site. We performed three docking procedures for each ligand and the best configuration of each of the ligand–receptor complexes was selected based on energetic grounds. The affinity scoring function δG was used to assess and rank the receptor–ligand complexes. The docking scores and the hydrogen bonding strength of all the molecules were shown in Table 2.

The synthesized series derivatives had dock score ranging from −12.4670 to −18.3979. Compound 4c-1 was showing the best least docking score of −18.3979 and the next best least docking score was found with 4d-1 followed by 4d-2. Two hydrogen bonds were present in the derivative 4a-1, 4b-1 and 4c-1, which was the highest among the series. Compound 4c-1 was found to be forming two hydrogen bonds of lengths 2.02 and 3.49 Å each with O of O–N in the oxime ester group and N in pyridine ring of Tyr27 respectively (Fig. 1). Compound 4d-1 only formed one hydrogen bond of length 3.03 Å with O–N in oxime ester group of Tyr27 (Fig. 2). Compound 4d-2 also formed only one hydrogen bond of bond length 2.87 Å with O–N in oxime ester group of Tyr27 (Fig. 3). The compounds 4c-1, 4d-1 and 4d-2 exhibited the best least docking score had good in vitro anti-HBV activity.

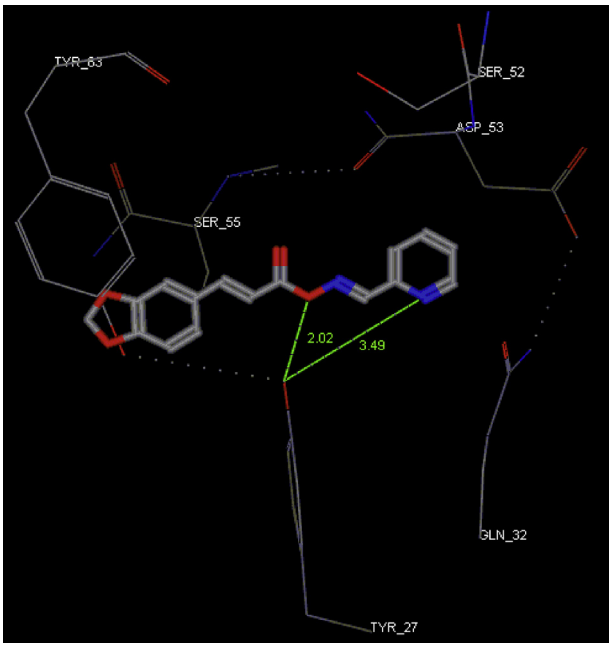

Fig. 1. Binding mode of 4c-1 into the binding site of HLA-A. The hydrogen bond formed colored in green. (For interpretation of the references to colour in this figure legend, the reader is referred to the web version of this article.)

Table 2
Docking score and bond interactions of synthesized compounds.

Ligand	S-score (kcal/mol)	No. of H-bonds	Distance (A)	Amino acid involved	Molecular structure
3TC	−10.7074	2	2.03	TYR 27	O of –OH
			2.29	TYR 27	O of –COC–
4a-1	−15.0037	2	1.77	TYR 27	O of –ON
			2.77	TYR 27	N of pyridine
4a-2	−14.1510	0	–	–	–
4a-3	−14.1436	1	2.67	TYR 27	O of –ON
4b-1	−16.5849	2	2.63	TYR 27	O of –ON
			3.39	TYR 27	N of pyridine
4b-2	−16.4346	1	2.98	TYR 27	O of –ON
4b-3	−16.4019	1	2.99	TYR 27	O of –ON
4c-1	−18.3979	2	2.02	TYR 27	O of –ON
			3.49	TYR 27	N of pyridine
4c-2	−12.5508	1	1.89	TYR 27	O of –ON
4c-3	−12.4670	1	1.90	TYR 27	O of –ON
4d-1	−16.6093	1	3.03	TYR 27	O of –ON
4d-2	−16.5985	1	2.87	TYR 27	O of –ON
4d-3	−14.8563	1	2.86	TYR 27	O of –ON

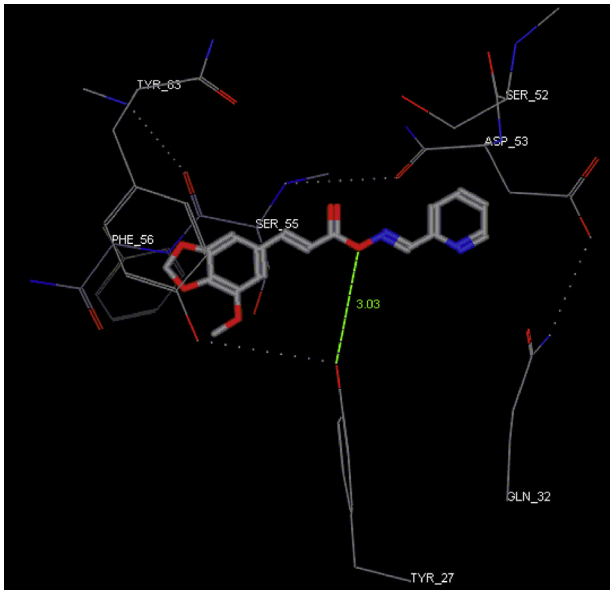

Fig. 2. Binding mode of 4d-1 into the binding site of HLA-A. The hydrogen bond formed colored in green. (For interpretation of the references to colour in this figure legend, the reader is referred to the web version of this article.)

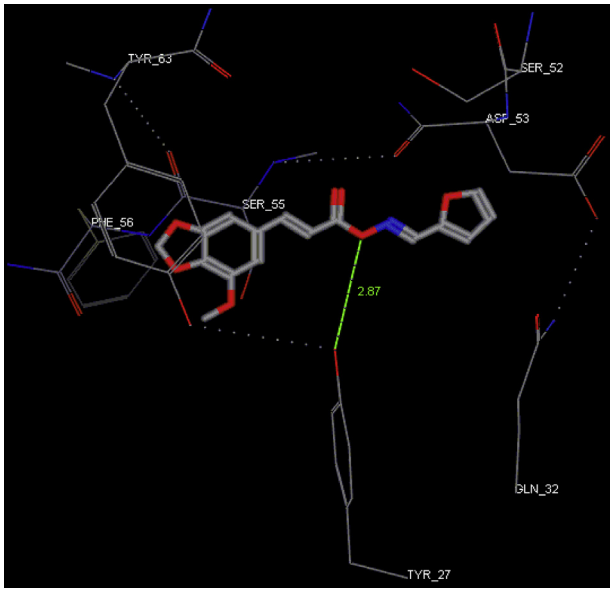

Fig. 3. Binding mode of 4d-2 into the binding site of HLA-A. The hydrogen bond formed colored in green. (For interpretation of the references to colour in this figure legend, the reader is referred to the web version of this article.)

2.4. Anti-HBV activity

All the newly synthesized derivatives were tested for their anti-HBV activity, namely inhibiting the secretion of HBsAg, and HBeAg in HepG 2.2.15 cells using lamivudine (3 TC, a clinically popular anti-HBV agent) as a positive control. The anti-HBV activity of each compound was expressed as the concentration of compound that achieved 50% inhibition (IC_{50}) to the secretion of HBsAg and HBeAg. And the cytotoxicity of each compound was expressed as the concentration of compound required to kill 50% (CC_{50}) of the HepG 2.2.15 cells. The selectivity index (SI), a major pharmaceutical parameter that estimates possible future clinical development, was determined as the ratio of CC_{50} to IC_{50}. The results of their anti-HBV activity and cytotoxicity were listed in Table 3.

The treatment of HBV-transfected HepG2.2.15 cells with various concentrations of drugs for 9 d exhibited a time-and dose-dependent inhibitory effect on the secretion of HBsAg and HBeAg (Fig. 4). In synthesized derivatives, all compounds showed better activity inhibiting the secretion of HBsAg than that of lamivudine. And eleven of twelve derivatives, with higher inhibitory activity against the secretion of HBeAg than lamivudine were obtained except for 4a-3. Compound 4c-1 showed the most potent anti-HBV activity, demonstrating potent inhibitory effect on the secretion of HBsAg ($IC_{50} = 14.08$ μM, SI = 17.85) and HBeAg ($IC_{50} = 6.20$ μM, SI = 40.82) but appeared toxic ($CC_{50} = 253.11$ μM). Compound 4d-1 showed the next most potent inhibitory to the secretion of HBsAg ($IC_{50} = 62.79$ μM) and HBeAg ($IC_{50} = 72.91$ μM). Compared to compound 4d-1, compound 4d-2 relatively low inhibitory potency to the secretion of HBsAg ($IC_{50} = 63.51$ μM) and HBeAg ($IC_{50} = 75.26$ μM), but weak toxic ($CC_{50} = 819.58$ μM) led to relatively high SI values ($SI_{HBsAg} = 12.90$, $SI_{HBeAg} = 10.89$).

Importantly, the most active compounds 4c-1, 4c-2, 4d-1, 4d-2 and 4d-3 with high activities against HBsAg and HBeAg were selected to investigate inhibition of HBV DNA replication using lamivudine as the reference drug. Compounds 4c-1, 4d-1, and 4d-2 exhibited anti-HBV activity with their IC_{50} values against HBV DNA replication of 23.43, 95.04, 139.73 μM, respectively. Compounds 4c-1, 4d-1, and 4d-2 displayed inhibiting not only HBsAg and HBeAg secretion but also HBV DNA replication, however, 3 TC showed significantly activity against HBV DNA replication ($IC_{50} = 6.86$) while showed little inhibitory on HBsAg and HBeAg secretion.

2.5. Structure–activity relationship

The start reactants substituted benzaldehyde 1a–d, intermediates 2a-d and oximes 1–3 showed low suppressant properties on the HBV while most of the derivatives showed high potency activity against of the secretion of HBsAg and HBeAg as shown in Table 3. In the docking study, we also found that the O of O–N in the oxime ester group interacted with Tyr27 by hydrogen bond. It indicated that oxime ester group (O=C–O–N=C) of the newly synthesized derivatives might be a good target for further lead optimization by introduction the rational substitutions.

Derivatives 4a-1 to 4d-1, 4a-2 to 4d-2 and 4a-3 to 4d-3 with the same oxime groups respectively showed different anti-HBV activity and cytotoxicity. Derivative 4d-2, with IC_{50} values of 63.51 μM and 75.26 μM for HBsAg and HBeAg respectively, was showing the most effective on inhibiting HBsAg and HBeAg secretion and the next was 4c-2 (HBsAg $IC_{50} = 64.60$ μM, HBeAg $IC_{50} = 81.83$ μM), followed by 4b-2 (HBsAg $IC_{50} = 173.31$ μM, HBeAg $IC_{50} = 189.67$ μM). It was similar to the derivatives 4a-1 to 4d-1 and 4a-3 to 4d-3 except that compound 4c-1 (HBsAg $IC_{50} = 14.18$ μM, HBeAg $IC_{50} = 6.20$ μM) was observed to show more effective on inhibiting HBsAg and HBeAg secretion than that of 4d-1 (HBsAg $IC_{50} = 62.79$ μM, HBeAg $IC_{50} = 72.91$ μM) for its high cytotoxicity. Thus, after methoxy group introduced to the 5-C of cinnamoyl group, the inhibitory effect of compounds 4b-1, 4b-2 and 4b-3 on secretion of HBsAg and HBeAg slightly increased comparing to compounds 4a-1, 4a-2 and 4a-3 respectively. The introduction of the methoxy group to 5-C of 4d-1, 4d-2, and 4d-3 could also increase their anti-HBV activity comparing to compounds 4c-1, 4c-2 and 4c-3 respectively. The substituent of 3,4-dimethoxy by 3,4-methylenedioxy could increase their inhibitory effect on secretion of HBsAg and HBeAg compared 4a-1~3 with 4c-1~3, and 4b-1~3 with 4d-1~3. Compound 4a-2 displayed more cytotoxicity ($CC_{50} = 624.24$ μM) than 4b-2 ($CC_{50} = 1049.90$ μM) and 4c-2 possessed higher cytotoxicity ($CC_{50} = 479.62$ μM) than 4d-2

Table 3
Anti-HBV activity and cytotoxicity of the phenylpropanoid derivatives in vitro[a].

Compd	CC_{50}[b] (μM)	HBsAg[c]		HBeAg[d]		DNA replication	
		IC_{50}[e] (μM)	SI[f]	IC_{50}[e] (μM)	SI[f]	IC_{50}[e] (μM)	SI[f]
1a	>1500	–[g]	–	–	–	ND[i]	ND
1b	>1500	–	–	–	–	ND	ND
1c	1289.31	–	–	–	–	ND	ND
1d	1075.75	–	–	–	–	ND	ND
2a	534.66	>600	<0.89	>600	<0.89	ND	ND
2b	834.13	>600	<1.39	>600	<1.39	ND	ND
2c	503.46	433.15	1.16	526.25	0.96	ND	ND
2d	667.25	410.96	1.62	476.75	1.40	ND	ND
1	402.02	387.17	1.04	469.11	0.86	ND	ND
2	475.21	479.80	1.01	519.47	0.91	ND	ND
3	562.19	353.56	1.59	431.23	1.30	ND	ND
4a-1	545.16	151.87	3.59	161.74	3.37	ND	ND
4a-2	624.24	191.26	3.26	201.65	3.10	ND	ND
4a-3	574.33	228.67	2.51	377.87	1.52	ND	ND
4b-1	787.32	142.67	5.52	150.08	5.25	ND	ND
4b-2	1049.90	173.31	6.06	189.67	5.54	ND	ND
4b-3	857.37	196.62	4.36	209.22	4.10	ND	ND
4c-1	253.11	14.18	17.85	6.20	40.82	23.43	10.80
4c-2	479.62	64.60	7.42	81.83	5.86	–	–
4c-3	265.78	75.75	3.51	117.67	2.26	ND	ND
4d-1	644.93	62.79	10.27	72.91	8.85	95.04	6.78
4d-2	819.58	63.51	12.90	75.26	10.89	139.73	5.87
4d-3	676.60	74.37	9.10	104.52	6.47	–	–
3TC[h]	568.25	234.70	2.42	267.16	2.13	6.86	82.84

[a] Values are means determined from at least two experiments.
[b] CC_{50} is 50% cytotoxicity concentration in HepG2 2.2.15 cells.
[c] HBsAg: hepatitis B surface antigen.
[d] HBeAg, hepatitis B e antigen.
[e] IC_{50} is 50% inhibitory concentration.
[f] SI (selectivity index) = CC_{50}/IC_{50}.
[g] No SI can be obtained.
[h] Lamivudine (3TC) as the positive control.
[i] ND, Not determined.

(CC_{50} = 819.58 μM), which indicated that the introduction of the methoxy group to 5-C could decrease cytotoxicity. Then, the cytotoxicity of 4c-2 was still stronger than that of 4a-2 and that of 4d-2 also stronger than 4b-2, indicating that the substituent of 3,4-dimethoxy by 3,4-methylenedioxy could increase the cytotoxicity. From the above results, it is indicated that the introduction of methoxy group to 5-C could enhance the anti-HBV activity and decrease cytotoxicity along with the high SI values, and the substituent of 3,4-dimethoxy by 3,4-methylenedioxy could increase activity and cytotoxicity along with relatively low SI values.

Derivatives 4a-1~3, 4b-1~3, 4c-1~3 and 4d-1~3 contained the same phenylpropanoid part respectively. 4a-1 showed the best anti-HBV activity (HBsAg IC_{50} = 151.87 μM, HBeAg IC_{50} = 161.74 μM) and the next was 4a-2 (HBsAg IC_{50} = 191.26 μM, HBeAg IC_{50} = 201.65 μM), followed by 4a-3 (HBsAg IC_{50} = 228.67 μM, HBeAg IC_{50} = 377.87 μM). The order also applied to 4b-1~3, 4c-1~3 and 4d-1~3. It suggested that the introduction of pyridine showed relatively high potent anti-HBV activity than introduction of furan and thiophene. Compound 4a-1 showed cytotoxicity with CC_{50} values of 545.16 μM. The cytotoxicity of derivatives 4a-3 (CC_{50} = 574.33 μM) decreased with thiophene group. Compound 4a-2 (CC_{50} = 624.24 μM) was observed with the weakest cytotoxicity with furan group. Actually, all the derivatives obtained from oxime 2 did show weakest cytotoxicity, followed by that from oxime 3. It indicated that the introduction of pyridine group could enhance the anti-HBV activity but increase the cytotoxicity.

According to the results mentioned above, SARs were summarized as followed: (1) 5-OCH_3-substituted compounds with methylenedioxy at 13,14-C could provide higher anti-HBV activity than other analogs. (1) The anti-HBV activity of oxime-substituted compounds could be pyridine-substituted > furan-substituted > thiophene-substituted.

3. Conclusion

In summary, our design and synthesis have led to a series of non-nucleoside anti-HBV agents by attaching of the oximes to cinnamic acids. Most of the derivatives displayed potent anti-HBV activity with the SI_{HBsAg} values from 2.51 to 12.90 and SI_{HBeAg} values from 1.52 to 27.92. Interestingly, compounds 4c-1, 4d-1, and 4d-2 displayed inhibiting not only HBsAg and HBeAg secretion but also HBV DNA replication, however, 3 TC showed significantly activity against HBV DNA replication. In addition, the docking study of the tested compounds inside the HLA-A protein active site was predicted using a moe-docking technique. The results of the in vitro anti-HBV activity study were consistent with the docking results indicating that the anti-HBV effect of the prepared compounds may exert its anti-HBV activity by inhibiting HLA-A. This study identified a new class of potent anti-HBV agents and offered valuable information for seeking non-nucleoside anti-HBV drug candidates.

4. Materials and methods

4.1. General

Melting points were determined using electrothermal melting point apparatus WRX-4 (Shanghai, China) and were uncorrected. MS spectra were run on a Finnigan LCQ Deca XP MAX mass spectrometer (Thermo Fisher, San Jose, CA, USA) equipped with an ESI source and an ion trap analyzer in the positive ion mode/in the negative ion. NMR spectra were recorded on Bruker AM 400 MHz

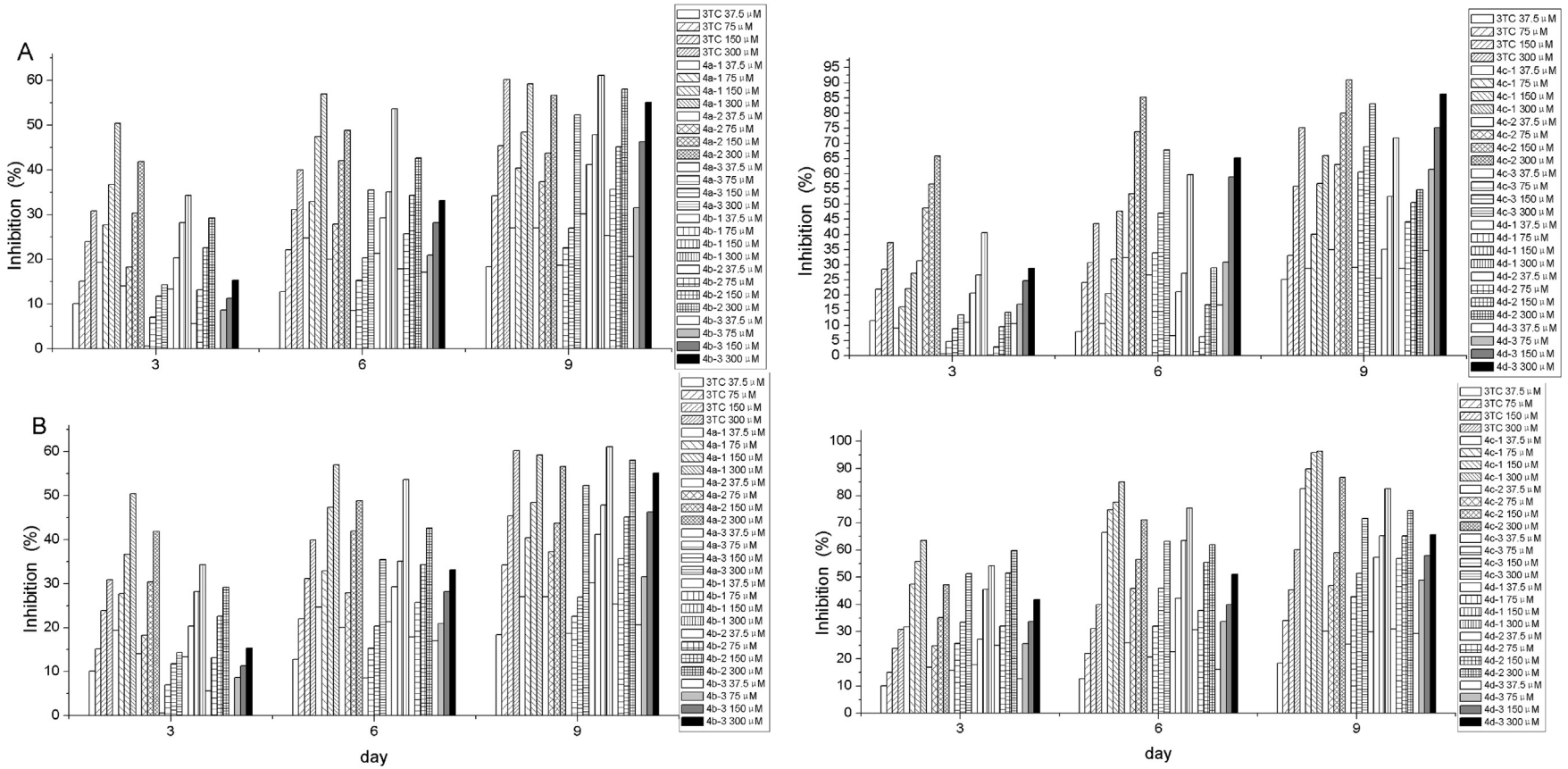

Fig. 4. Inhibitory effect of the phenylpropanoid derivatives on secretion of HBsAg (A) and HBeAg (B) in the HepG2.2.15 cell line. Data were expressed as mean ± S.D. ($n = 3$).

($^1H/^{13}C$, 400 MHz/100 MHz) or Bruker DRX 500 MHz ($^1H/^{13}C$, 500 MHz/125 MHz) spectrometer (Bruker, Bremerhaven, Germany) and chemical shifts were quoted in δ as parts per million (ppm) downfield with tetramethylsilane (TMS) as internal reference. Coupling constants, J, are expressed in hertz (Hz). Column chromatography (CC): silica gel (200–300 mesh; Qingdao Makall Group Co., Ltd; Qingdao; China). All reactions were monitored using thinlayer chromatography (TLC) on silica gel plates. On the basis of NMR and HPLC (Thermo Fisher UltiMate 3000, USA) data, all final compounds reported in the manuscript are >95% pure.

4.2. Chemistry (Scheme 1)

4.2.1. General procedure for preparation of compounds 2a–d

A mixture of compound 1 (1 equiv, 10 mmol), malonic acid (1.2 equiv, 12 mmol) and two drops of piperidine in pyridine (25 mL) was refluxed for 4 h and evaporated to remove pyridine. The residue was suspended in H_2O (30 mL) and extracted with EtOAc (2 × 50 mL) which was further purified by recrystallization to afford 2a-d.

4.2.1.1. (E)-3-(3,4-dimethoxyphenyl)acrylic acid (2a). Yield 82%. m.p. 181–183 °C. ESIMS: *m/z* 208.0600 $[M]^+$, calc. for $C_{11}H_{12}O_4$ (208.21) [27].

4.2.1.2. (E)-3-(3,4,5-trimethoxyphenyl)acrylic acid (2b). Yield 90%. m.p. 126–127 °C. ESIMS: *m/z* 238.6 $[M]^+$, 237.6 $[M-H]^+$, calc. for $C_{12}H_{14}O_5$ (238.24) [28].

4.2.1.3. (E)-3-(benzo[d][1,3]dioxol-5-yl)acrylic acid (2c). Yield 85%. m.p. 242–244 °C. ESIMS: *m/z* 192.2 $[M]^+$, 408.4 $[2M + Na]^+$, calc. for $C_{10}H_8O_4$ (192.17) [29].

4.2.1.4. (E)-3-(7-methoxybenzo[d][1,3]dioxol-5-yl)acrylic acid (2d). Yield 80%. m.p. 228–229 °C. ESIMS: *m/z* 221 $[M-H]^+$, calc. for $C_{11}H_{10}O_5$ (222.19) [30].

4.2.2. General procedure for preparation of cinnamoyl chlorides 4a–d

Substituted cinnamoyl chlorides were obtained by refluxing for 5 h the appropriate acid 2a-d (10 mmol) with thionyl chloride (10 ml). After evaporation under reduced pressure, the crude liquid residue was used for subsequent reactions without purification.

4.2.3. General procedure for preparation of compounds 1–3

Hydroxylamine hydrochloride (1.2 equiv, 12 mmol) and sodium acetate (1.2 equiv, 12 mmol) were added to a solution of the aldehyde (1 equiv, 10 mmol) in EtOH (50 ml). The reaction was stirred at 60 °C for 2 h. After the EtOH was remove evaporated in vacuo, the residue was suspended in DCM (50 ml) and washed with 1 M HCl solution (3 × 30 ml), H_2O (3 × 30 ml) and brine solution. The organic phase was dried (Na_2SO_4) and then concentrated at reduced pressure. The oximes 1–3 were purified by recrystallization.

4.2.3.1. Picolinaldehyde oxime (1). Yield 100%. m.p. 112–113 °C. ESIMS: *m/z* 123.1 $[M+H]^+$, calc. for $C_6H_6N_2O$ (122.12) [31].

4.2.3.2. Furan-2-carbaldehyde oxime (2). Yield 99%. m.p. 88–89 °C. ESIMS: *m/z* 112.1 $[M+H]^+$, calc. for $C_5H_5NO_2$ (111.1) [32].

4.2.3.3. Thiophene-2-carbaldehyde oxime (3). Yield 100%. m.p. 130–132 °C. ESIMS: *m/z* 128.1 $[M+H]^+$, calc. for C_5H_5NOS (127.16) [33].

4.2.4. General procedure for preparation of compounds 4a-1~4d-3

Oxime (1 equiv, 10 mmol) was resolved in dry DCM (20 ml) and then triethylamine (TEA) (1.2 equiv, 12 mmol) was added drop wise to the solution at 0 °C and then reaction mixture was stirred for 30 min at 0 °C. Appropriate acid chloride (1 equiv, 10 mmol) was added to the mixture and then reaction mixture was stirred for 10–20 min at 0 °C, for 12 h at room temperature. DCM was evaporated to dryness. The residue was washed with cold ether (5 ml) and hot water and then purified by column chromatography on silica gel eluting with ethyl acetate/petroleum ether 1:1to 3:1.

4.2.4.1. (E)-Picolinaldehyde O-3-(3,4-dimethoxyphenyl)acryloyl oxime (4a-1). White crystal, yield 67%. m.p. 147.0–147.3 °C. ^1H NMR (500 MHz, $CDCl_3$): δ 3.94 (6H, each 3H, s, H-16, 17), 6.45 (1H, d, J = 15.91, H-8), 6.90 (1H, d, J = 8.30, H-5), 7.11 (1H, d, J = 1.94, H-2), 7.18 (1H, dd, J = 1.94, 8.30, H-6), 7.38 (1H, ddd, J = 1.00, 1.63, 4.88, H-13), 7.78 (1H, td, J = 1.63, 7.91, H-14), 7.84 (1H, d, J = 15.91, H-7), 8.17 (1H, d, J = 7.91, H-15), 8.54 (1H, s, H-10), 8.68 (1H, dd, J = 4.88, H-12). ^{13}C NMR (125 MHz, CDCl3): δ 164.59 (C-9), 156.61 (C-10), 151.59 (C-11), 150.12 (C-3), 149.87 (C-12), 149.27 (C-4), 146.85 (C-7), 136.68 (C-14), 127.13 (C-1), 125.41 (C-13), 123.11 (C-15), 122.10 (C-6), 112.57 (C-8), 111.06 (C-5), 109.77 (C-2), 56.00, 55.92 (C-16, 17). DEPT135: δ 164.31, 153.49, 150.02, 140.61, 129.58 (C), 156.73, 149.86, 146.90, 136.76, 125.49, 122.5, 105.54 (CH), 61.00, 56.20 (CH_3). ESIMS: *m/z* 313.798 $[M+H]^+$, 336.021 $[M+Na]^+$, 648.812 $[2M + H + Na]^+$, calc. for $C_{17}H_{16}N_2O_4$ (312.32).

4.2.4.2. (E)-Furan-2-carbaldehyde O-3-(3,4-dimethoxyphenyl) acryloyl oxime (4a-2). White crystal, yield 53%. m.p. 169.5.1–169.9 °C. ^1H NMR (500 MHz, $CDCl_3$): δ 3.96 (6H, each 3H, s, H-15, 16), 6.52 (1H, d, J = 15.90, H-8), 6.53 (1H, q, J = 1.75, 3.50, H-13), 7.01 (1H, d, J = 8.25, H-5), 7.13 (1H, d, J = 1.95, H-2), 7.16 (1H, d, J = 3.50, H-12), 7.17 (1H, d, J = 15.90, H-7), 7.21 (1H, dd, J = 1.95, 8.25, H-6), 7.47(1H, d, J = 1.75, H-14), 8.76 (1H, s, H-10). ^{13}C NMR (125 MHz, $CDCl_3$): δ 164.99 (C-9), 158.65 (C-10), 150.82 (C-3), 149.56 (C-11), 149.45 (C-4), 146.30 (C-7), 144.40 (C-14), 130.67 (C-1), 119.81(C-6), 115.23 (C-8), 112.34 (C-13), 111.78 (C-5), 110.48 (C-2), 109.49 (C-12), 56.12, 56.07 (C-15, 16). ESIMS: *m/z* 301.4 $[M^+]$, calc. for $C_{16}H_{15}NO_5$ (301.29).

4.2.4.3. (E)-Thiophene-2-carbaldehyde O-3-(3,4-dimethoxyphenyl) acryloyl oxime (4a-3). White crystal, yield 60%. m.p. 135.8–136.3 °C. ^1H NMR (400 MHz, $CDCl_3$): δ 3.95 (6H, each 3H, s, H-15, 16), 6.39 (1H, d, J = 15.90 Hz, H-8), 6.86(1H, d, J = 6.81 Hz, H-5), 7.00 (1H, d, J = 1.53 Hz, H-2), 7.19 (1H, dd, J = 1.53, 6.81, Hz, H-6), 7.13 (1H, t, J = 4.22, 4.49 Hz, H-13), 7.55 (1H, d, J = 4.49 Hz, H-14), 7.56 (1H, d, J = 4.22 Hz, H-12), 7.74 (1H, d, J = 15.90 Hz, H-7), 8.35 (1H, s, H-10). ^{13}C NMR (100 MHz, $CDCl_3$): δ 165.01 (C-9), 158.88 (C-10), 150.91 (C-3), 149.74 (C-4), 146.18 (C-7), 144.32 (C-11), 129.35 (C-1), 127.81 (C-12), 127.15 (C-13), 126.20 (C-14), 121.24 (C-6), 114.31 (C-8), 110.54 (C-5), 109.83 (C-2), 56.80, 56.46 (C-15, 16). ESIMS: *m/z* 318.138 $[M+H]^+$, 659.570 $[2M + Na]^+$, calc. for $C_{16}H_{15}NO_4S$ (317.36).

4.2.4.4. (E)-Picolinaldehyde O-3-(3,4,5-trimethoxyphenyl)acryloyl oxime (4b-1). White crystal, yield 58%. m.p. 121.1–121.3 °C. ^1H NMR (500 MHz, $CDCl_3$): δ 3.91 (9H, each 3H, s, H-16, 17, 18), 6.48 (1H, d, J = 15.85, H-8), 6.82 (2H, s, H-2, 6), 7.39 (1H, ddd, J = 1.10, 2.62, 4.94, H-13), 7.80 (1H, td, J = 2.62, 7.92, H-14), 7.83 (1H, d, J = 15.85, H-7), 8.18 (1H, dm, J = 1.10, 7.92, H-15), 8.56 (1H, s, H-10), 8.69 (1H, m, J = 4.94, H-12). ^{13}C NMR (125 MHz, $CDCl_3$): δ 164.31 (C-9), 156.73 (C-10), 153.49 (C-11), 150.02 (C-3, 5), 149.86 (C-12), 146.90 (C-7), 140.61 (C-4), 136.76 (C-14), 129.58 (C-1), 125.49 (C-13), 122.15 (C-15), 114.20 (C-8), 105.54 (C-2, 6), 61.00 (C-17), 56.20 (C-16, 18). DEPT135: δ 164.31, 153.49, 150.02, 140.61, 129.58 (C), 156.73, 149.86, 146.90, 136.76, 125.49, 122.5, 105.54 (CH), 61.00, 56.20 (CH_3).

ESIMS: *m/z* 343.1296 $[M+H]^+$, 365.1115 $[M+Na]^+$, calc. for $C_{18}H_{18}N_2O_5$ (342.35).

4.2.4.5. (E)-Furan-2-carbaldehyde O-3-(3,4,5-trimethoxyphenyl) acryloyl oxime (4b-2). White crystal, yield 59%. m.p. 102.6–102.9 °C. ^{1}H NMR (500 MHz, $CDCl_3$): δ 3.89 (9H, each 3H, s, H-15, 16, 17), 6.43 (1H, q, J = 1.95, 3.60, H-13), 6.70 (1H, d, J = 15.28, H-8), 6.74 (2H, s, H-2, 6), 6.83 (1H, d, J = 3.60, H-12), 7.47(1H, d, J = 1.95, H-14), 7.62 (1H, d, J = 15.28, H-7), 8.36 (1H, s, H-10). ^{13}C NMR (125 MHz, $CDCl_3$): δ 165.66 (C-9), 159.59 (C-10), 153.43 (C-3, 5), 149.56 (C-11), 146.90 (C-7), 142.39 (C-14), 139.56 (C-4), 129.75 (C-1), 115.56 (C-8), 112.37 (C-13), 109.41 (C-12), 105.10 (C-2, 6),60.97 (C-16), 55.26 (C-15, 17). ESIMS: *m/z* 332.1207 $[M+H]^+$, 354.1031 $[M+Na]^+$, calc. for $C_{17}H_{17}NO_6$ (331.32).

4.2.4.6. (E)-Thiophene-2-carbaldehyde O-3-(3,4,5-trimethoxyphenyl) acryloyl oxime (4b-3). White crystal, yield 51%. m.p. 142.5–142.9 °C. ^{1}H NMR (500 MHz, $CDCl_3$): δ 3.90 (9H, each 3H, s, H-15, 16, 17), 6.48 (1H, d, J = 15.85, H-8), 6.82 (2H, s, H-2, 6), 7.13 (1H, q, J = 4.91, 5.61 Hz, H-13), 7.56 (1H, d, J = 5.61 Hz, H-14), 7.58 (1H, d, J = 4.91 Hz, H-12), 7.82 (1H, d, J = 15.85, H-7), 8.37 (1H, s, H-10). ^{13}C NMR (125 MHz, $CDCl_3$): δ 165.92 (C-9), 159.34 (C-10), 153.24 (C-3, 5), 146.59 (C-7), 144.32 (C-11), 140.47 (C-4), 129.29 (C-1), 128.03 (C-12), 127.80 (C-13), 125.84 (C-14), 115.28 (C-8), 105.46 (C-2, 6),60.76 (C-16), 56.69 (C-15, 17). ESIMS: *m/z* 370.3 $[M+Na]^+$, calc. for $C_{17}H_{17}NO_5S$ (347.39).

4.2.4.7. (E)-Picolinaldehyde O-3-(benzo[d][1,3]dioxol-5-yl)acryloyl oxime (4c-1). White crystal, yield 52%. m.p. 157.0–157.3 °C. ^{1}H NMR (500 MHz, $CDCl_3$): δ 6.02 (2H, s, H-16), 6.45 (1H, d, J = 15.25, H-8), 6.92 (1H, d, J = 7.50, H-5), 7.09 (1H, dd, J = 1.84, 7.50, H-6), 7.21 (1H, d, J = 1.84, H-2), 7.26 (1H, ddd, J = 1.38, 4.75, 5.29, H-13), 7.71 (1H, td, J = 5.29, 7.49, H-14), 7.79 (1H, d, J = 15.25, H-7), 8.18 (1H, d, J = 7.49, H-15), 8.56 (1H, s, H-10), 8.60 (1H, d, J = 4.75, H-12). ^{13}C NMR (125 MHz, $CDCl_3$): δ 162.31 (C-9), 155.15 (C-10), 150.54 (C-11), 149.86 (C-12), 149.44 (C-3), 149.16 (C-4), 146.89 (C-7), 136.58 (C-14), 126.53 (C-1), 125.11 (C-13), 123.95 (C-15), 122.77 (C-6), 114.28 (C-8), 109.15 (C-5), 106.88 (C-2), 101.49 (C-16). DEPT135: δ 162.31, 150.54, 149.44, 149.16, 126.53 (C), 155.15, 149.86, 146.89, 136.58, 125.11, 123.95, 122.77, 114.28, 109.15, 106.88 (CH),101.49 (CH_2). ESIMS: *m/z* 297 $[M+H]^+$, 319 $[M+Na]^+$, calc. for $C_{16}H_{12}N_2O_4$ (296.28).

4.2.4.8. (E)-Furan-2-carbaldehyde O-3-(benzo[d][1,3]dioxol-5-yl) acryloyl oxime (4c-2). White crystal, yield 49%. m.p. 157.8–158.0 °C. ^{1}H NMR (500 MHz, $CDCl_3$): 6.03 (2H, s, H-15), 6.37 (1H, d, J = 15.86 Hz, H-8), 6.53 (1H, q, J = 1.80, 3.48, H-13), 6.85(1H, d, J = 8.02 Hz, H-5), 7.06 (1H, dd, J = 1.56, 8.02 Hz, H-6), 7.09 (1H, d, J = 1.56 Hz, H-2), 7.17 (1H, dd, J = 0.79, 3.48 Hz, H-12), 7.48 (1H, dd, J = 0.79, 1.80 Hz, H-14), 7.77 (1H, d, J = 15.86 Hz, H-7), 8.36 (1H, s, H-10). ^{13}C NMR (125 MHz, $CDCl_3$): δ 165.22 (C-9), 157.39 (C-10), 149.90 (C-3), 149.41 (C-11), 148.06 (C-4), 146.47 (C-7), 144.41 (C-14), 129.49 (C-1), 119.46(C-6), 115.25 (C-8), 112.35 (C-13), 110.64 (C-5), 109.90 (C-2), 109.15 (C-12), 101.60 (C-15). ESIMS: *m/z* 308.2 $[M+Na]^+$, calc. for $C_{15}H_{11}NO_5$ (285.25).

4.2.4.9. (E)-Thiophene-2-carbaldehyde O-3-(benzo[d][1,3]dioxol-5-yl)acryloyl oxime (4c-3). White crystal, yield 57%. m.p. 139.6–139.9 °C. ^{1}H NMR (500 MHz, $CDCl_3$): δ 6.02 (2H, s, H-15), 6.40 (1H, d, J = 15.57 Hz, H-8), 6.86(1H, d, J = 7.76 Hz, H-5), 7.01 (1H, dd, J = 1.22, 7.76 Hz, H-6), 7.10 (1H, q, J = 4.13, 5.67 Hz, H-13), 7.12 (1H, d, J = 1.22 Hz, H-2), 7.52 (1H, d, J = 5.67 Hz, H-14), 7.54 (1H, d, J = 4.13 Hz, H-12), 7.69 (1H, d, J = 15.57 Hz, H-7), 8.36 (1H, s, H-10). ^{13}C NMR (125 MHz, $CDCl_3$): δ 164.75 (C-9), 158.34 (C-10), 149.80 (C-3), 148.84 (C-4), 146.35 (C-7), 143.46 (C-11), 129.31 (C-1), 127.81 (C-12), 127.01 (C-13), 125.06 (C-14), 121.13 (C-6), 114.79 (C-8), 109.95 (C-5), 106.50 (C-2), 101.56 (C-15). ESIMS: *m/z* 301.1480 $[M^+]$, 323.1103 $[M+Na]^+$, calc. for $C_{15}H_{11}NO_4S$ (301.32).

4.2.4.10. (E)-Picolinaldehyde O-3-(7-methoxybenzo[d][1,3]dioxol-5-yl)acryloyl oxime (4d-1). White crystal, yield 58%. m.p. 186.3–186.6 °C. ^{1}H NMR (500 MHz, $CDCl_3$): δ 3.95 (3H, s, H-17), 6.04 (2H, s, H-16), 6.42 (1H, d, J = 15.89, H-8), 6.77 (1H, d, J = 1.25, H-6), 6.82 (1H, d, J = 1.25, H-2), 7.39 (1H, m, J = 1.74, 6.89, H-13), 7.79 (1H, td, J = 1.40, 7.92, H-14), 7.77 (1H, d, J = 15.89, H-7), 8.17 (1H, d, J = 7.92, H-15), 8.55 (1H, s, H-10), 8.69 (1H, dd, J = 4.42, H-12). ^{13}C NMR (125 MHz, CDCl3): δ 164.46 (C-9), 156.60 (C-10), 150.04 (C-11), 149.80 (C-12), 149.46 (C-5), 146.71 (C-7), 143.75 (C-3), 137.88 (C-4), 136.82 (C-14), 128.95 (C-1), 125.48 (C-13), 122.17 (C-15), 113.39 (C-8), 109.69 (C-6), 101.49 (C-2), 102.12(C-16), 56.67 (C-17). DEPT135: δ 164.46, 150.04, 149.46, 143.75, 137.88, 128.95 (C), 156.60, 149.80, 146.71, 136.82, 125.48, 122.17, 113.39, 109.69, 101.49 (CH), 102.12 (CH_2), 56.67 (CH_3). ESIMS: *m/z* 327.0987 $[M+H]^+$, 349.0807 $[M+Na]^+$, calc. for $C_{17}H_{14}N_2O_5$ (326.3).

4.2.4.11. (E)-Furan-2-carbaldehyde O-3-(7-methoxybenzo[d][1,3]dioxol-5-yl)acryloyl oxime (4d-2). White crystal, yield 64%. m.p. 122.5–122.8 °C. ^{1}H NMR (500 MHz, $CDCl_3$): δ 3.94 (3H, s, H-16), 6.03 (2H, s, H-15), 6.39 (1H, d, J = 15.85 Hz, H-8), 6.92 (1H, d, J = 1.36 Hz, H-6), 7.01 (1H, d, J = 1.36 Hz, H-2), 6.52 (1H, q, J = 1.75, 3.45 Hz, H-13), 7.17(1H, dd, J = 0.80, 3.45 Hz, H-12), 7.47 (1H, d, J = 0.80, 1.75, H-16), 7.75 (1H, d, J = 15.85 Hz, H-7), 8.36 (1H, s, H-10). ^{13}C NMR (125 MHz, CDCl3): δ 165.00 (C-9), 159.37 (C-10), 150.49 (C-5), 149.33 (C-11), 146.58 (C-7), 144.17 (C-14), 143.24 (C-3), 136.80 (C-4), 128.75 (C-1), 115.18 (C-8), 112.33 (C-13), 109.92(C-6),109.56 (C-12), 101.60 (C-15), 101.45 (C-2), 56.44 (C-16). ESIMS: *m/z* 338.3423 $[M+Na]^+$, calc. for $C_{16}H_{13}NO_6$ (315.28).

4.2.4.12. (E)-Thiophene-2-carbaldehyde O-3-(7-methoxybenzo[d][1,3]dioxol-5-yl)acryloyl oxime (4d-3). White crystal, yield 61%. m.p. 132.6–133.2 °C. ^{1}H NMR (500 MHz, $CDCl_3$): δ 3.92 (3H, s, H-16), 6.00 (2H, s, H-15), 6.67(1H, d, J = 1.18 Hz, H-2), 6.74 (1H, d, J = 15.28 Hz, H-8), 6.75(1H, d, J = 1.18 Hz, H-6), 6.93 (1H, d, J = 3.97 Hz, H-12), 7.17 (1H, q, J = 3.97, 4.72 Hz, H-13), 7.19 (1H, d, J = 4.72 Hz, H-14), 7.53 (1H, d, J = 15.28 Hz, H-7), 8.36 (1H, s, H-10). ^{13}C NMR (125 MHz, $CDCl_3$): δ 164.36 (C-9), 160.04 (C-10), 149.29 (C-5), 146.41 (C-7), 143.61 (C-3),142.09 (C-11), 136.58 (C-4), 130.38 (C-1), 127.80 (C-12), 127.59 (C-13), 126.07 (C-14), 115.93 (C-8), 109.04 (C-6), 101.82 (C-15), 100.70 (C-2), 56.69 (C-16). DEPT135: δ 164.36, 149.29, 143.61, 136.58, 130.38 (C), 160.04, 146.41, 142.09, 127.80, 127.59, 126.07, 115.93, 109.04, 100.70 (CH), 101.82 (CH_2), 56.69 (CH_3). ESIMS: *m/z* 332.4 $[M+H]^+$, 354 $[M+Na]^+$, calc. for $C_{16}H_{13}NO_5S$ (331.34).

4.3. Molecular docking studies

The ligand study was carried out by HyperChem software, a sophisticated molecular modeling environment that uniting with quantum chemical calculations, dynamics, and molecular mechanics [34]. Three-dimensional structures were constructed and optimized for all the molecules, and then QSAR descriptors were studied, which is a powerful lead optimization tool that can quantitatively relate variations in biological activity to changes in molecular properties.

In our previous studies, niranthin, nirtetralin, nirtetralin A and nirtetralin B from *P. niruri* L. were confirmed to possess anti-HBV activity [10–12]. Then we investigated the potential anti-HBV targets of the anti-HBV constituents with reverse docking approach using fifteen HBV related proteins and RNA including human leukocyte antigen HLA-A*02:03 (PDB ID: 3OX8), human leukocyte antigen HLAA*02:06 (PDB ID: 3OXR), human leukocyte antigen HLA-A*02:07 (PDB ID: 3OXS), hepatitis B virus preS1 protein (PDB

ID: 3ZHF), hepatitis B virus preS2 surface antigen (PDB ID: 1WZ4), human hepatitis B virus surface antigen HzKR127 (PDB ID: 2EH8), human hepatitis B virus e-antigen (PDB ID: 3V6F, 3V6Z), Hepatitis B X-interacting protein HBXIP (PDB ID: 3MS6, 4WZR, 4WZW), HBV RNA polymerase (PDB ID: 2HN7), and human hepatitis B virus encapsidation signal (PDB ID: 2IXY, 2K5Z). HLA-A protein (PDB ID: 3OX8) showed the best reverse docking result and was chosen as molecular target for further docking study.

The molecular docking study was performed using MOE 2008.10 to understand the ligand–protein interactions in detail. The target compounds were built using the builder interface of the MOE program and subjected to energy minimization. The crystal structure of human leukocyte antigen (HLA-A) protein (PDB ID: 3OX8) was retrieved from Protein Data Bank (http://www.rcsb.org/pdb/home/home.do) [35]. The edited crystal structure after removing water molecules was imported into MOE and chain A was considered for docking process as the protein is a dimer consisting of A and B chains. The structure is protonated, polar hydrogens were added and energy minimization was carried out till the gradient convergence 0.05 kcal/mol was reached to get the stabilized conformation. The active site was correlated with 'Site Finder' module of MOE to define the docking site for the ligands. Docking procedure was followed using the standard protocol implemented in MOE 2008.10 and the geometry of resulting complexes was studied using the MOE's Pose Viewer utility.

4.4. Pharmacology

4.4.1. Cells and cell culture

HepG2.2.15 (clonal cells derived from human hepatoma cell line G2) cells were provided by the Chinese Academy of Medical Sciences (P.R. China) and maintained in MEM medium supplemented with 10% fetal bovine serum and 380 μg/ml of G418, 50 u/ml of kanamycin, and 0.03% L-glutamine at 37 °C in a 5% CO_2 atmosphere with 100% humidity.

4.4.2. Drug treatment

HepG 2.2.15 cells were seeded at a density of 1×10^5 cells/ml (200 μl/well) in 96-well plates and maintained at 37 °C for 24 h prior to extract addition, followed by treatment with various concentrations of drugs. Lamivudine (3 TC) was served as the positive control. Cells were refed with drug-containing fresh medium every 3 d for up to 9 d in time-dependent experiment. Medium was taken at third day of treatment (T3), the sixth day of treatment (T6) and the ninth day of treatment (T9), and stored at −20 °C until analysis. The IC_{50} and selected index (SI) of each compound were calculated, respectively.

4.4.3. Cell toxicity

Logarithmically growing cells were seeded in 96-well culture plates at a density of 1×10^5 cells/ml (200 μl/well). They were cultured for 24 h and then treated with various concentrations of drugs. OD values were read at 450 nm after 9days and the percent of cell death was calculated and the cells were refed with drug-containing fresh medium every 3 d for up to 9 d. After drug treatment, the cytotoxicity was measured using the MTT assay [36,37].

4.4.4. Determination of HBsAg and HBeAg

The levels of HBV surface antigen (HBsAg) and HBV e antigen (HBeAg) were simultaneously detected using ELISA kits (Rongsheng Biotechnology Co. Ltd, Shanghai, China) according to the manufacturer's instructions.

4.4.5. Determination of HBV replication

Inhibitory activity against HBV was determined by a real-time fluorescence quantitative PCR (FQ-PCR) according to our previous description [11]. Briefly, 2.0 μl HBV DNA was amplified in a 25 mL mixture containing 12.5 μl 2 × SYBR Green Master (ROX) and 2 primers specific for HBV: a forward primer (5′-AAC CAT TGA AGC AAT CAC TAG AC-3′) and a reverse primer (5′- ATC TAT GGT GGC TGC TCG AAC TA -3′). The thermal program comprised of an initial denaturation at 95 °C for 10 min followed by 40 amplification cycles with each of the two following steps: 95 °C for 15 s and 60 °C for 1 min.

Acknowledgments

This work was financially supported by the National Natural Science Foundation of China (No. 81060261), Natural Science Foundation of Guangxi Province, China, (No. 2011jjD20002), and science research and technology development foundation of Guagnxi province, China (No.11107009-3-5).

Appendix A. Supplementary data

Supplementary data related to this article can be found at http://dx.doi.org/10.1016/j.ejmech.2015.03.056.

References

[1] N. Gitilin, HepatitisB: diagnosis, prevention and treatment, Clin. Biochem. 43 (1997) 1500–1506.
[2] M. Rizzetto, A. Ciancio, Chronic HBV-related liver disease, Mol. Asp. Med. 29 (2008) 72–84.
[3] D. Lavanchy, Hepatitis B virus epidemiology, disease burden, treatment, and current and emerging prevention and control measures, J. Viral Hepat. 11 (2004) 97–107.
[4] K. Sato, M. Mori, Current and novel therapies for Hepatitis B virus infection, Mini-Rev. Med. Chem. 10 (2010) 20–31.
[5] C.X. Ying, Y. Li, C.H. Leung, M.D. Robek, Y.C. Cheng, Unique antiviral mechanism discovered in anti-hepatitis B virus research with a natural product analogue, Proc. Natl. Acad. Sci. U. S. A. 104 (2007) 8526–8531.
[6] L.M. Gao, Y.X. Han, Y.P. Wang, Y.H. Li, Y.Q. Shan, X. Li, Z.G. Peng, C.W. Bi, T. Zhang, N.N. Du, J.D. Jiang, D.Q. Song, Design and synthesis of oxymatrine analogues overcoming drug resistance in hepatitis B virus through targeting host heat stress cognate 70, J. Med. Chem. 54 (2011) 869–876.
[7] I.T. Crosby, D.G. Bourke, E.D. Jones, T.P. Jeynes, S. Cox, J.A.V. Coates, A.D. Robertson, Antiviral agents 3. Discovery of a novel small molecule non-nucleoside inhibitor of Hepatitis B Virus (HBV), Bioorg. Med. Chem. Lett. 21 (2011) 1644–1648.
[8] N.N. Du, X. Li, Y.P. Wang, F. Liu, Y.X. Liu, C.X. Li, Z.G. Peng, L.M. Gao, J.D. Jiang, D.Q. Song, Synthesis, structure-activity relationship and biological evaluation of novel N-substituted matrinic acid derivatives as host heat-stress cognate 70 (Hsc70) down-regulators, Bioorg. Med. Chem. Lett. 21 (2011) 4732–4735.
[9] L.J. Wang, C.A. Geng, Y.B. Ma, X.Y. Huang, J. Luo, H. Chen, R.H. Guo, X.M. Zhang, J.J. Chen, Synthesis, structure–activity relationships and biological evaluation of caudatin derivatives as novel anti-hepatitis B virus agents, Bioorgan. Med. Chem. 20 (2012) 2877–2888.
[10] W.X. Wei, X.R. Li, K.W. Wang, Z.W. Zheng, M. Zhou, Lignans with anti-hepatitis B virus activities from Phyllanthus niruri L, Phytother. Res. 26 (2012) 964–968.
[11] S. Liu, W.X. Wei, K.C. Shi, X. Cao, M. Zhou, Z.P. Liu, In vitro and in vivo anti-hepatitis B virus activities of the lignan niranthin isolated from Phyllanthus niruri L, J. Ethnopharmacol. 155 (2014) 1061–1067.
[12] S. Liu, W.X. Wei, Y.B. Li, X. Lin, K.C. Shi, X. Cao, M. Zhou, In vitro and in vivo anti-hepatitis B virus activities of the lignan nirtetralin B isolated from Phyllanthus niruri L, J. Ethnopharmacol. 157 (2014) 62–68.
[13] C. Viegas-Junior, A. Danuello, V.D. Bolzani, E.J. Barreir, C.A.M. Fraga, Molecular hybridization: a useful tool in the design of new drug prototypes, Curr. Med. Chem. 14 (2007) 1829–1852.
[14] H. Chen, Y.B. Ma, X.Y. Huang, C.A. Geng, Y. Zhao, L.J. Wang, R.H. Guo, W.J. Liang, X.M. Zhang, J.J. Chen, Synthesis, structure–activity relationships and biological evaluation of dehydroandrographolide and andrographolide derivatives as novel anti-hepatitis B virus agents, Bioorg. Med. Chem. Lett. 24 (2014) 2353–2359.
[15] Z.R. Wu, L.F. Zheng, Y. Li, F. Su, X.X. Yue, W. Tang, X.Y. Ma, J.Y. Nie, H.Y. Li, Synthesis and structure–activity relationships and effects of phenylpropanoid amides of octopamine and dopamine on tyrosinase inhibition and anti-oxidation, Food Chem. 134 (2012) 1128–1131.
[16] S.N. Kim, J.Y. Lee, H.J. Kim, C.G. Shin, H. Parka, Y.S. Lee, Synthesis and HIV-1 integrase inhibitory activities of caffeoylglucosides, Bioorg. Med. Chem. Lett. 10 (2000) 1879–1882.

[17] P. Panda, M. Appalashetti, M. Natarajan, C.P. Mary, S.S. Venkatraman, Z.M.A. Judeh, Synthesis and antiproliferative activity of helonioside A,3′,4′,6′-tri-O-feruloylsucrose, lapathoside C and their analogs, Eur. J. Med. Chem. 58 (2012) 418–430.
[18] P. Panda, M. Appalashetti, M. Natarajan, M.B. Chan-Park, S.S. Venkatraman, Z.M.A. Judeh, Synthesis and antitumor activity of lapathoside D and its analogs, Eur. J. Med. Chem. 53 (2012) 1–12.
[19] F. Zhang, G. Wang, A review of non-nucleoside anti-hepatitis B virus agents, Eur. J. Med. Chem. 75 (2014) 267–281.
[20] Y.K. Zhang, H.Y. Zhong, Z.L. Lv, M.F. Zhang, T. Zhang, Q.S. Li, K. Li, Anti-hepatitis B virus and anti-cancer activities of novel isoflavone analogs, Eur. J. Med. Chem. 62 (2013) 158–167.
[21] L. Roux, S. Priet, N. Payrot, C. Weck, M. Fournier, F. Zoulim, J. Balzarini, B. Canard, K. Alvarez, Ester prodrugs of acyclic nucleoside thiophosphonates compared to phosphonates: synthesis, antiviral activity and decomposition study, Eur. J. Med. Chem. 63 (2013) 869–881.
[22] F.D. Santos, P. Abreu, H.C. Castro, I.C.P.P. Paixao, C.C. Cirne-Santos, V. Giongo, J.E. Barbosa, B.R. Simonetti, V. Garrido, D.C. Bou-Habib, D.D. Silva, P.N. Batalha, J.R. Temerozo, T.M. Souza, C.M. Nogueira, A.C. Cunha, C.R. Rodrigues, V.F. Ferreira, M.C.B.V. de Souza, Synthesis, antiviral activity and molecular modeling of oxoquinoline derivatives, Bioorgan. Med. Chem. 17 (2009) 5476–5481.
[23] K.R. Babu, V.K. Rao, Y.N. Kumar, K. Polireddy, K.V. Subbaiah, M. Bhaskar, V. Lokanatha, C.N. Raju, Identification of substituted [3, 2-a] pyrimidines as selective antiviral agents: molecular modeling study, Antivir. Res. 95 (2012) 118–127.
[24] V.V. Quan, C. Trenerry, S. Rochfort, J. Wadeson, C. Leyton, A.B. Hughes, Synthesis and anti-inflammatory activity of aromatic glucosinolates, Bioorgan. Med. Chem. 21 (2013) 5945–5954.
[25] H.B. Zou, H. Wu, X.N. Zhang, Y. Zhao, S. Joachim, Y.J. Lou, Y.P. Yu, Synthesis, biological evaluation, and structure-activity relationship study of novel cytotoxic aza-caffeic acid derivatives, Bioorgan. Med. Chem. 18 (2010) 6351–6359.
[26] A. Karakurt, A.A.B.S. Mehmet, Ü. Çalıs, S. Dalkara, Synthesis of some novel 1-(2-naphthyl)-2-(imidazol-1-yl)ethanone oxime ester derivatives and evaluation of their anticonvulsant activity, Eur. J. Med. Chem. 57 (2012) 275–282.
[27] R. David Brittelli, Phosphite-mediated in situ carboxyvinylation: a new general acrylic acid synthesis, J. Org. Chem. 46 (1981) 2514–2520.
[28] M.W. Klohs, M.D. Draper, F. Keller, Alkaloids of Rauwolfia serpentina. III. Rescinnamine, a new hypotensive and sedative principle, J. Am. Chem. Soc. 76 (1954) 2843.
[29] M.L. Salum, C.J. Robles, R. Erra-Balsells, Photoisomerization of ionic liquid ammonium cinnamates: one-pot synthesis-isolation of Z-cinnamic acids, Org. Lett. 12 (2010) 4808–4811.
[30] A.H. Salway, Synthesis of substances allied to cotarnine, J. Chem. Soc. Trans. 95 (1909) 1204–1220.
[31] E.J. Poziomek, B.E.J. Hackley, G.M. Steinberg, Pyridinium aldoximes, J. Org. Chem. 23 (1958) 714–717.
[32] J. Nidhi, K. Anil, S.M.S. Chauhan, Metalloporphyrin and heteropoly acid catalyzed oxidation of CNOH bonds in an ionic liquid: biomimetic models of nitric oxide synthase, Tetrahedron Lett. 46 (2005) 2599–2602.
[33] L. Fernando, D.L.C. Pilar, E. Eva, G.C. Araceli, D.L.H. Antonio, L.A. Vicente, Synthesis and properties of Isoxazolo[60]fullerene-Donor Dyads, J. Org. Chem. 65 (2000) 8675–8684.
[34] S. Dastmalchi, M. Hamzeh-Mivehroud, T. Ghafourian, H. Hamzeiy, Molecular modeling of histamine H3 receptor and QSAR studies on arylbenzofuran derived H3 antagonists, J. Mol. Graph. Model 26 (2008) 834–844.
[35] J.X. Liu, Y. Kenneth, E.C.R. Chen, Structural insights into the binding of Hepatitis B virus core peptide to HLA-A2 alleles: towards designing better vaccines, Eur. J. Immunol. 41 (2011) 2097–2106.
[36] M. Ferrari, M.C. Fornasiero, A.M. Isetta, MTT colorimetric assay for testing macrophage cytotoxic activity in vitro, J. Immunol. Methods 131 (1990) 165–172.
[37] Y.Q. Han, Z.M. Huang, X.B. Yang, H.Z. Liu, G.X. Wu, In vivo and in vitro anti-hepatitis B virus activity of total phenolics from Oenanthe javanica, J. Ethnopharmacol. 118 (2008) 148–153.